Continuous wave and pulsed EPR measurements of chromium-doped fluoro-chlorozirconate and fluoro-bromozirconate glasses

1997 J. Phys.: Condens. Matter 9 9175

(http://iopscience.iop.org/0953-8984/9/43/004)

J. Phys.: Condens. Matter **9** (1997) 9175–9185. Printed in the UK PII: S0953-8984(97)81725-0

Continuous wave and pulsed EPR measurements of chromium-doped fluoro-chlorozirconate and fluoro-bromozirconate glasses

J I Martínez, M A Buñuel, R Cases and P J Alonso

Instituto de Ciencia de Materiales de Aragón, (Consejo Superior de Investigaciones Científicas—Universidad de Zaragoza), Plaza S Francisco s/n, 50009 Zaragoza, Spain

Received 10 February 1997, in final form 24 June 1997

Abstract. A continuous wave (CW) and pulsed electron paramagnetic resonance (EPR) investigation of chromium-doped fluoro-chlorozirconate and fluoro-bromozirconate glasses with different contents of the heaviest halogens is presented. The CW EPR spectra are interpreted by assuming a preferential substitution of the fluoride ions in the first co-ordination shell of the Cr^{3+} ions by chloride or bromide ions, which is in agreement with previous optical data. Values for the spin Hamiltonian parameters are discussed for different amounts of halide substitution. Pulsed EPR studies are mainly focused on the ESEEM (electron spin echo envelope modulation) signal. It shows the frequency peaks due to fluoride ions and to the corresponding alkali metal cation (Na or Li), which provides information about the bulk structure of the glass and strongly suggests that it is essentially the same as that of the fluorozirconate glasses. ESEEM results indicate that Cr^{3+} centres are mainly isolated.

1. Introduction

Since their discovery in the mid-seventies [1], heavy metal fluoride glasses (HMFG) have received great attention because of their potential applications as active optical materials [2]. These glasses show a wide optical window ranging from the near-ultraviolet to the middle-infrared region and have low optical losses; their phonon energies are lower than those of the oxide glasses and they can incorporate variable amounts of rare earths and transition metal ions as active centres for different optical applications. HMFG ZrF_4 based glasses (fluorozirconate glasses) have been widely studied and, in particular, the characterization of the optical properties of fluorozirconate glasses doped with 3d ions has received considerable attention in recent years [3–5]. One of the most promising aspects of the doped glasses is the quantum yield of the emissions, which is higher for HMFGs than for oxide glasses because of the lower value of the local vibration energies that leads to lower values for the multiphonon non-radiative de-excitation probabilities.

It is known that if fluorides are substituted by heavier halide ions (chlorides or bromides) the phonon frequencies will decrease along with the multiphonon non-radiative de-excitation probabilities resulting in an enhancement of the quantum yield of the emissions. Unfortunately, chlorozirconate and bromozirconate glasses cannot be used in practice because of their low chemical stability mainly due to attack by atmospheric water and because of their greater tendency to de-vitrification.

In order to overcome these difficulties, fluoro-chlorozirconate and fluoro-bromozirconate glasses have appeared more recently. These glasses basically consist of fluorozirconate

0953-8984/97/439175+11$19.50

glasses in which a small fraction (typically up to 10%) of the fluoride ions are substituted by chloride or bromide ions [6]. A number of studies on the structure of these mixed glasses using different techniques indicate that the local structure in the vicinity of the Zr^{4+} ion is hardly affected while the heavy halide anions occupy non-bridging sites [7–9]. The chemical stability and the glass stability against de-vitrification are bulk properties, thus the low amount of heavier halides has no appreciable influence on them. On the other hand, it has been found that the refractive index increases as a consequence of the incorporation of more polarizable anions [6]. In addition, the optical properties of the active ions (rare earths or 3d ions) are greatly affected, opening a new way for the preparation of glasses with promising applications [10–13].

In particular, the optical properties (absorption, emission and lifetime measurements) of Cr^{3+}, Ni^{2+} and Mn^{2+} in fluoro-chlorozirconate and fluoro-bromozirconate glasses have been studied in our laboratory. The changes in the optical properties associated with the 3d ion as a function of chlorine or bromine content are interpreted assuming that the metal forms hexaco-ordinate complexes and the heavier halides preferentially occupy a neighbouring site to the active impurity in such a way that the optical properties of the doped glasses are due to the existence of metal ions co-ordinated to n F^- and $(6-n)$ X^- (X = Cl or Br) where n can be 6, 5, 3, 1, 0 [11–13]. Extended x-ray absorption fine structure (EXAFS) studies [14] of the nickel environment in fluoro-chlorozirconate glasses confirm this interpretation.

As long as the active impurities are paramagnetic ions, additional structural information can be obtained from continuous wave and pulsed electron paramagnetic resonance (CW EPR and pulsed EPR respectively) measurements. CW EPR spectra are very sensitive to the co-ordination geometry of the paramagnetic species in the sample. Pulsed EPR, and in particular the electron spin echo envelope modulation (ESEEM) technique, is a powerful tool for investigating weak interactions of the paramagnetic entity with matrix nuclei with a non-zero nuclear spin [15].

Bearing these ideas in mind, we have undertaken a study, by CW EPR and ESEEM techniques, of several series of chromium-doped fluoro-chlorozirconate and fluoro-bromozirconate glasses with different concentrations of chlorine and bromine ions. Harris [16] has reported the CW EPR spectra of chromium-doped fluorozirconate glasses, which were interpreted by considering that Cr^{3+} ions are placed in distorted fluorine octahedra and the existence of chromium exchange-coupled clusters is also pointed out. Legein *et al* [17, 18] have also studied the CW EPR spectra of Cr^{3+} ions in a number of transition metal fluoride glasses. Simulations of the Cr^{3+} CW EPR spectra carried out by these authors proved that such clusters are not needed to explain their EPR results. Instead, a suitable distribution of crystal field parameters can account for the observed spectra. As far as ESEEM studies are concerned, ours is, to the best of our knowledge, the first of this kind on halide glasses and, since the ESEEM signal is associated with weak interacting nuclei, it would provide useful information about the bulk distribution of the anions in the mixed glasses.

2. Experimental details

Multicomponent glasses were prepared as described in [13]. The starting compositions (in mol%) of the chromium-doped fluorozirconate glasses were 52 ZrF_4, 20 BaF_2, (21-c) MF (M = Na or Li), 4.5 LaF_3, 2.5 AlF_3 and c CrF_3 where c ranges from 0.10 to 0.20. Mixed halide glasses were prepared using appropriate quantities of BaX_2 and/or NaX (X=Cl or Br) instead of the corresponding amount of BaF_2 and/or MF (M=Na or Li). The starting compositions were therefore 52 ZrF_4, (20-x) BaF_2, x BaX_2, (21-y-c) MF, y NaX, 4.5 LaF_3,

2.5 AlF_3 and c CrF_3. The samples were labelled as ZCr(c)X(x, y) in the case of mixed halide glasses and as ZCr(c) in the case of fluorozirconate samples. In this way, the starting concentration of the substitute halogen X is $(2x + y)/(290 + 2c)$ (see table 1).

Table 1. Chemical composition of the mixed halide glasses used in this work.

			X concentration $\times 100$	
Sample	X	M	Starting	Actual
ZCr(0.10)Cl(5.0, 0.0)	Cl	Li	3.45	0.93
ZCr(0.20)Cl(0.0, 7.5)	Cl	Na	2.58	2.06
ZCr(0.10)Cl(15.0, 0.0)	Cl	Li	10.34	2.32
ZCr(0.10)Cl(3.5, 3.0)	Cl	Na	3.45	2.34
ZCr(0.15)Cl(7.5, 9.0)	Cl	Na	8.27	7.39
ZCr(0.15)Br(2.5, 0.0)	Br	Na	1.72	1.23
ZCr(0.10)Br(15.0, 0.0)	Br	Li	10.34	1.28
ZCr(0.15)Br(20.0, 0.0)	Br	Li	13.78	2.32
ZCr(0.15)Br(5.0, 6.0)	Br	Na	5.51	5.76

The actual composition of the samples was obtained by elemental microanalysis with an electron probe using an SEM (scanning electron microscope) JEOL JSM 6400. The electron energy was 20 keV and measurements were performed with a probe current of 0.6 nA. Table 1 also summarizes the results obtained.

CW EPR and pulsed EPR measurements were performed using a Bruker ESP380E spectrometer in the X band. The measurements were taken at different temperatures between 6 K and room temperature (RT) using an Oxford CF935 continuous cryostat refrigerated with liquid helium. A TWT tube was used as a microwave amplifier for the pulsed EPR measurements. The three-pulse, $\pi/2$–τ–$\pi/2$–τ'–$\pi/2$, sequence (hereafter 3p sequence) was used. The width of the $\pi/2$ pulses was adjusted to 16 ns. Suitable phase cycling was performed to eliminate unwanted echoes. The decay of the echo amplitude was sampled with a 32 ns time interval and typical measurements consist of 256 data points.

3. Experimental results

3.1. CW EPR

X-band EPR spectra of chromium-containing fluoro-chlorozirconate and fluoro-bromozirconate glasses with different concentrations of chloride and bromide ions have been measured at different temperatures between 6 K and RT. Hardly any differences in the CW EPR were found on varying the temperature.

As a starting point, we shall consider a chromium-doped fluorozirconate glass; sample ZCr(0.15). The EPR spectrum of such a sample (figure 1(a)) is similar to that reported by Harris [16] and Legein *et al* [17, 18]. It shows two main features at different magnetic field positions. In the field region extending from 130 to 170 mT (corresponding to g values between 6 and 5) an intense peak is seen. It shows a sharp edge at $g \approx 6$, a maximum at about $g = 5.5$ and falls and becomes smoother when the field increases. In the region around $g = 2$ (at about 340 mT) a peak derivative is observed. This feature has long tails, especially in the high-field region. Some structure in the region at about 300 mT is also seen. Following previous studies [16–18] these signals are assigned to Cr^{3+} centres.

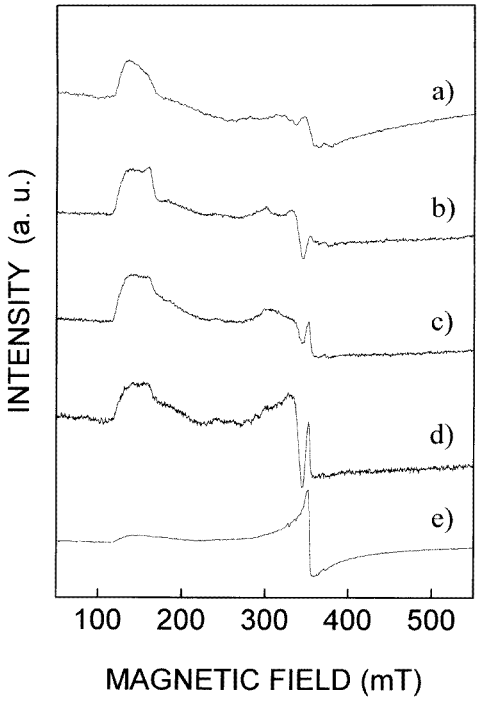

Figure 1. X-band (9.5 GHz) CW EPR spectra of chromium-doped fluoro-chlorozirconate glasses of different compositions measured at RT. (a) Pure ZCr(0.15) fluorozirconate glass. (b) ZCr(0.10)Cl(5.0, 0.0), (c) ZCr(0.20)Cl(0.0, 7.5), (d) ZCr(0.10)Cl(15.0, 0.0) and (e) ZCr(0.15)Cl(7.5, 9.0) samples.

We shall now describe the results obtained from samples with chloride and bromide ions separately.

3.1.1. Fluoro-chlorozirconate glasses. The CW EPR spectra of chromium-doped fluoro-chlorozirconate glasses with different chloride ion concentrations are shown in figure 1, traces b to e. We find basically the same features as present in the ZCr(0.15) sample spectrum. In some of the samples (traces b, c, d) two new signals at $g \approx 4.3$ and $g \approx 2$ (this latter at slightly lower field than the high-field part of the Cr^{3+} signal) are detected. This new features do not appear to be correlated with chromium or chlorine concentrations and are attributed to Fe^{3+} impurities, that had been detected in the synthesis compounds. As far as the Cr^{3+} signal is concerned, the increasing of the chlorine concentration causes changes in the relative intensities of the spectral features. The high-field part of the spectrum ($g \approx 2$) becomes more intense for higher chlorine concentrations. The effect is specially marked for samples with the highest chlorine concentrations (about 7%, figure 1(e)).

3.1.2. Fluoro-bromozirconate glasses. The CW EPR spectra of chromium-doped fluoro-bromozirconate with different bromide ion contents are shown in figure 2. For the purpose of comparison, the spectrum corresponding to the fluorozirconate glass ZCr(0.15) has also been included (trace a). For low bromide ion content (traces b, c) the differences between the spectra of fluoro-bromozirconate glasses and that of fluorozirconate glass are minor (see

figure 2, b and c). For a higher-bromine-content sample (trace d), the EPR spectrum seems to show similar features to the fluoro-chlorozirconate sample (trace 1(d)), that is to say, an increase of the intensity of the resonance line in the $g = 2$ region with respect to that of the low-field region. Nevertheless, it has to be said that for the bromide sample, the resonance at $g \approx 2$ is much narrower than for the chloride sample. Finally, the spectrum of the highest-bromide-ion-concentration sample (trace e) shows a broad line near $g = 2$ that could be the envelope of all features shown in the other samples for this magnetic field region. In summary, the evolution of the EPR spectra of fluoro-bromozirconate samples with the bromide ion content is not so clear as for the fluoro-chlorozirconate ones.

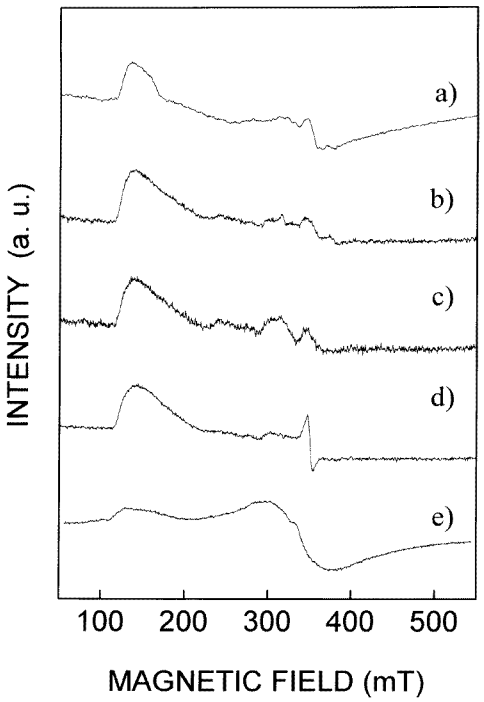

Figure 2. X-band (9.5 GHz) CW EPR spectra of chromium-doped fluoro-bromozirconate glasses for different compositions measured at RT. (a) Pure ZCr(0.15) fluorozirconate glass. (b) ZCr(0.15)Br(2.5, 0.0), (c) ZCr(0.10)Br(15.0, 0.0), (d) ZCr(0.15)Br(20.0, 0.0) and (e) ZCr(0.15)Br(5.0, 6.0) samples.

3.2. Pulsed EPR measurements

Chromium-doped mixed glass samples show a measurable electron spin echo (ESE) signal when excited with a suitable pulse sequence at low enough temperatures. We measured, at 6 K, the evolution of the stimulated ESE intensity caused by excitation with a 3p sequence as a function of the delay time, τ', between the second and third pulses. The ESE decay shows some oscillations (ESEEM signal) which are due to the superhyperfine (shf) interaction of the Cr^{3+} with the magnetic nuclei in the sample when the shf interactions are anisotropic. The frequencies of these oscillations correspond to the nuclear splitting in the electronic spin manifolds among which the EPR transition takes place. In glassy samples there are paramagnetic centres in all possible orientations and so, in principle, modulations at sharp

frequencies are not obtained [15]. This problem can be simplified by fixing the magnetic field in a position where only centres in determined orientations contribute to the EPR signal. This technique is called the orientation-selective experiment [19]. In our case, we can select a single orientation measuring at a field very close to the low-field edge of the CW EPR spectra (figures 1 and 2).

In this manner, we obtained our ESEEM signal using a dc magnetic field intensity of 130 mT for all the samples. The echo signal was very weak, but one-dimensional 3p pulse echo decays could be measured in all cases. Changes in the chloride and bromide ion content of the mixed glasses do not produce any effect. As an example, in figure 3 we show the results obtained for the ZCr(0.15)Cl(7.5, 9.0) sample. The ESE decays are extremely fast and the decay time is estimated to be about 2 μs in all cases. However, the modulation frequencies depend on the alkali metal, Na or Li, present in the sample. In order to obtain the frequency spectra, a sixth-order polynomial function was subtracted to account for the unmodulated ESE decay component, and a fast Fourier transform algorithm was used to obtain the ESEEM frequency spectra from the remaining modulated contribution. In the case of glasses with lithium (figure 4(a)), two peaks at 5.2 MHz and 2.1 MHz with similar intensities are observed when the time interval, τ, between the first two pulses of the exciting 3p sequence is set to 144 ns. When the ESE decays of glasses with sodium are measured under the same conditions, the corresponding ESEEM frequency spectra again show the peak at 5.2 MHz, but the one at 2.1 MHz disappears and a much less intense peak at about 1.4 MHz is observed (figure 4(b)).

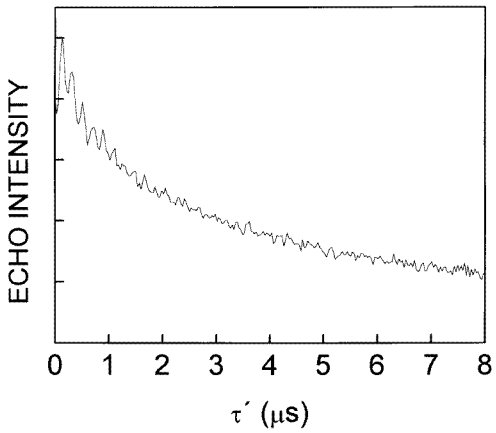

Figure 3. Decay of the 3p induced echo ($\tau = 144$ ns) measured at 6 K with a dc magnetic field of 130 mT, in ZCr(0.15)Cl(7.5, 9.0) glass.

4. Discussion

Except for the signals attributed to Fe^{3+} impurities, all the CW EPR spectra can be understood as being due to isolated Cr^{3+} ions in a distorted octahedral environment (chromium is co-ordinated to six halide ions). This is in agreement with the interpretation given by Legein *et al* [17, 18] for EPR measurements of fluorozirconate glasses with similar concentrations of Cr^{3+}. Its electronic spin is $S = 3/2$. The corresponding spin Hamiltonian is [16, 17]:

$$H = g\mu_B \boldsymbol{B} \cdot \boldsymbol{S} + D\{S_z^2 - \tfrac{1}{3}S(S+1)\} + E(S_x^2 - S_y^2) \qquad (1)$$

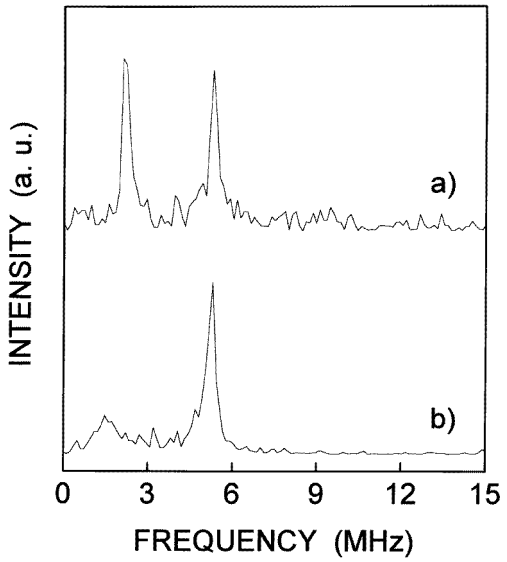

Figure 4. Frequency spectra obtained by Fourier transform of the ESEEM signal measured at 6 K with a dc magnetic field of 130 mT and $\tau = 144$ ns (a) in the lithium-containing ZCr(0.15)Br(20.0, 0.0) glass and (b) in the sodium-containing ZCr(0.15)Cl(7.5, 9.0) glass.

where an isotropic Zeeman term and an orthorhombic zero-field contribution are included. μ_B is the Bohr magneton, g the isotropic g factor and D and E are the axial and rhombic zero-field parameters respectively.

Simulation of the CW EPR spectra of $S = 3/2$ systems has been performed by Legein *et al* [17, 18] for different values of the zero-field parameters. For systems in which $D > g\mu_B B$ and the E/D ratio has small values, the EPR spectrum shows a resonance in the $g \approx 5$ region (corresponding to the 'forbidden' $|+3/2\rangle \longleftrightarrow |-3/2\rangle$ transition in the *parallel* orientation), an accumulation point at $g \approx 2.0$ and some signals spreading over a large range from $g \approx 2$ to high field. Their results demonstrate that our measurements can be described using the spin Hamiltonian (1). The spectrum of pure fluorozirconate glass are similar to those simulated by Legein *et al* [17, 18] with a distribution of D values centred around 18 GHz. The spectrum of our glass with maximum chlorine substitution is very similar to that simulated by Legein *et al* [18] considering a distribution of D values centred around 9 GHz. In fact, the evolution of EPR measurements with the chlorine concentration in the sample is compatible with a continuous decreasing of the D values. The evolution of the spectra with bromine concentration is not conclusive. It has to be taken into account that our spectra are due to a complicated distribution of Cr^{3+} centres, both in the geometry and in the number of substituted ligand halogens. This could explain the differences between our measured spectra and Legein's simulations.

Changes in D values are due to variations in distance and covalence of the halogen–chromium bonds. As mentioned above, Legein's simulations rule out the requirement of exchange-coupled chromium clusters in the sample for explanation of the EPR spectra, as had been postulated by other authors [16] for fluorozirconate glasses.

Following previous studies [11, 14] that point to a glass structure in which it is mainly the fluoride ions co-ordinated to chromium that are substituted by chloride or bromide ions, we consider the spectra corresponding to heavily substituted glasses (figures 1(a), 1(e) and

2(e)) as arising from samples in which chromium is co-ordinated only octahedrally, with the six corners occupied by one kind of anion (F^- in the fluorozirconate glass and Cl^- and Br^- in the corresponding mixed glasses). Optical spectroscopy studies performed by Buñuel *et al* [12, 13] are in agreement with this interpretation. The mentioned studies also indicate that in all the other mixed glasses the Cr^{3+} neighbourhoods are octahedral and combine different numbers of fluoride and substitute halide ions, then the EPR spectra can be considered as a superposition of signals from Cr^{3+} in these different environments.

As a final comment on the CW EPR of Cr^{3+} in these mixed halide glasses it would be interesting to compare the changes of the most probable values of the zero-field parameter, D, when fluoride ions are substituted by chloride or bromide ions, with the corresponding modifications of the optical properties [12, 13].

These optical properties have been described assuming an octahedral environment for the active ion. The ground state of the free Cr^{3+} ion is ^4F and, in octahedral symmetry, it is split into two triplets, $^4T_{1g}$ and $^4T_{2g}$, and a singlet, $^4A_{2g}$, the ground state. The energy difference between the ground state and the first excited state, $^4T_{2g}$, is the crystal field splitting Δ. If an axial distortion takes place, this first excited state is further split into a singlet and a doublet ($^4B_{2g}$ and ^4E_g if the point symmetry is D_{4h}) with δ being the energy separation between them.

Using the perturbative standard analysis of the magnetic properties of an orbital singlet in an intermediate crystal field [20] and assuming that $\delta \ll \Delta$, in agreement with the optical properties analysis [12, 13], it is found that

$$g_\parallel = g_e - 8\frac{\lambda}{\Delta} - \frac{16}{3}\frac{\lambda}{\Delta}\frac{\delta}{\Delta} \qquad g_\perp = g_e - 8\frac{\lambda}{\Delta} + \frac{8}{3}\frac{\lambda}{\Delta}\frac{\delta}{\Delta} \tag{2}$$

where g_e is the free electron g factor ($g_e = 2.0023$) and λ the spin–orbit coupling parameter. Then

$$D = -4\left(\frac{\lambda}{\Delta}\right)^2 \delta. \tag{3}$$

So, the anisotropy of the g tensor, $\delta g = g_\parallel - g_\perp$, is related to the zero-field parameter, D, by

$$\delta g = g_\parallel - g_\perp = -8\frac{\lambda}{\Delta}\frac{\delta}{\Delta} = 2\frac{D}{\lambda}. \tag{4}$$

From the optical data Buñuel [13] estimated the crystal field splitting, Δ, and the spin–orbit coupling parameter for the different *octahedral* Cr^{3+} ions where different fluoride ions are substituted by chloride or bromide ions. Buñuel obtains the values $\Delta = 15\,250\ cm^{-1}$ and $\lambda = 750\ cm^{-1}$ ($\lambda/\Delta = 4.9\times10^{-2}$) for fluorine hexaco-ordinated Cr^{3+} and $\Delta = 13\,700\ cm^{-1}$ and $\lambda = 600\ cm^{-1}$ ($\lambda/\Delta = 4.4\times10^{-2}$) and $\Delta = 13\,100\ cm^{-1}$ and $\lambda = 510\ cm^{-1}$ ($\lambda/\Delta = 3.9\times10^{-2}$) are associated with Cr^{3+} hexaco-ordinated with chloride or bromide ions respectively.

It is interesting to note that the expected values of the g-tensor anisotropy deduced from the D values (see equation (4)) will be too low to be detected in CW EPR spectra, and this is in agreement with our results. With respect to the splitting of the $^4T_{2g}$ excited triplet as a consequence of the low-symmetry distortion of the chromium neighbourhood, and since the values of λ/Δ are practically the same in all the cases, the decrease in the value of D from the $(CrF_6)^{3-}$ complex to the $(CrCl_6)^{3-}$ indicates that such splitting, δ, decreases when fluoride ions are substituted by chloride ions. Consequently, the ratio δ/Δ also decreases. This could be interpreted as the distortion of the Cr^{3+} ion environment remaining lower for the heavier halides.

Let us now discuss the pulsed EPR results and, because we are dealing with a disordered system [15], pay particular attention to the ESEEM signal that is due to weakly interacting nuclei. F, Cl, Br, Na, Li, Ba, La and Al all have isotopes with a non-zero nuclear spin and so, in principle, they could contribute to the echo decay modulation signal.

The analysis of the ESEEM signal due to weakly interacting nuclei in disordered solids is well established for $S = 1/2$ systems [15]. In our case, we are dealing with a Cr^{3+} ion which is an $S = 3/2$ system and, as mentioned previously, the echo decay is measured with a d.c. magnetic field in the low-field region of the EPR spectrum (about 130 mT), that is to say, exciting the $|+3/2\rangle \longleftrightarrow |-3/2\rangle$ forbidden transition of the *parallel* centres. For the zero-field splitting values quoted above, this transition within the Kramers doublet $|\pm 3/2\rangle$ is the only one which is excited and it is well separated from the other EPR Cr^{3+} transitions. Following the reasoning of Oliete *et al* [21], in that situation the ESEEM signal can be described using the $S = 1/2$ formalism. If the quadrupolar contribution that can appear if $I \geqslant 1$ is neglected, the ESEEM signal due to a weakly interacting nucleus with a nuclear spin I in a 3p experiment can be described by [15]

$$V_{3p}(\tau, \tau') = 1 - \frac{4}{5}\frac{b^2}{\omega_I^2} I(I+1)\{1 - \cos(\omega_I \tau)\}\{1 - F[b(\tau + \tau')]\cos[\omega_I(\tau + \tau')]\} \tag{5}$$

where b is the dipolar contribution to the shf interaction, ω_I is the nuclear Larmor frequency of the interacting nucleus and

$$F(x) = \frac{15}{4}\int_0^{\pi} \sin^2\theta \cos^2\theta \cos\left\{\frac{x}{2}(3\cos^2\theta - 1)\right\} \sin\theta \, \mathrm{d}\theta \tag{6}$$

accounts for the spatial averaging of the interacting nucleus around the electronic spin. This averaging is responsible for the additional decay of the modulation, which is faster than that of the unmodulated contribution to the echo decay.

Equation (5) indicates that only the nuclear Larmor frequency, ω_I, appears in the 3p echo decay modulation signal when the time, τ', between the last two pulses is varied. Moreover, the intensity of the modulation is driven by the factor $\{1 - \cos(\omega_I \tau)\}$ and so the choice of the time between the first two pulses, τ, is important in order to prevent suppression effects. The factor $\{1 - \cos(\omega_I \tau)\}$ must also be considered when making comparisons between the intensities of the modulated components of the echo decay due to different nuclei.

In principle, if the nucleus has an electric quadrupolar moment ($I \geqslant 1$) then the quadrupolar interaction also has to be taken into account. This interaction modifies the nuclear splitting and nuclear wavefunction in each electronic manifold. By comparison of the quadrupolar contribution with the nuclear Larmor frequency we can distinguish between weak- and strong-quadrupolar-interaction limits [15]. In the first case, the 3p ESEEM signal only gives the same modulation frequency, ω_I, and an extra decay is introduced as a consequence of the quadrupolar interaction. On the other hand, if this interaction becomes stronger, a splitting in the frequency spectrum of the ESEEM signal would appear as a consequence of the quadrupolar interaction.

Our ESEEM results can be explained by considering all these factors. The peak at 5.2 MHz in our ESEEM spectra (see figures 4(a) and 4(b)) corresponds to the Larmor frequency of ^{19}F ($I = 1/2$, 100% natural abundance) at 130 mT. This signal comes from the very weak interaction between the fluorine nuclei and the chromium electronic spin through a (dipolar) magnetic hyperfine term. The contribution of such remote fluorine nuclei to the spectrum is small, but the peak is intense because of the great quantity of remote fluorine nuclei in the sample. The peaks at 2.1 MHz (figure 4(a)) and 1.4 MHz (figure 4(b)) correspond to Larmor frequencies of ^7Li ($I = 3/2$, 92.5% natural abundance)

and ^{23}Na ($I = 3/2$, 100% natural abundance), respectively, and are also due to remote (weakly interacting) alkali metal nuclei. Other Larmor frequency peaks are not present provided that the other nuclei have a low concentration in the sample. Peaks corresponding to strongly interacting nuclei, such as fluorine, chlorine or bromine in the first co-ordination shell, are not observed. It is possible that the interactions of these nuclei were too strong to give an ESEEM peak and, on the other hand, their corresponding shf splittings cannot be seen in the CW EPR signal because they are hidden in the broad chromium feature.

At first glance the great intensity of the ^{7}Li peak at 2.1 MHz seems surprising in comparison with the ^{19}F peak. Lithium is fifteen times less abundant in the sample than fluorine nuclei. The intensity of the Larmor peak depends on the concentration of each nucleus in the sample, but also on the time, τ, between the first and second pulses in the ESEEM experiment as well as on the dipolar contribution to the shf interaction. The expression for the peak intensity has a multiplicative coefficient $I(I + 1)$ (see equation 5). Taking into account the nuclear spin of the alkali metal compared with that of the ^{19}F nucleus (see above), the contribution of the alkali metals to the ESEEM signal is five times as intense as that of the halogen. The rest of the intensity differences can be understood from the effect of distance between remote nuclei. The contribution of every nucleus to the peak is driven by dipolar interaction. This means (see equation (5)) that the main contribution to the intensity comes from nuclei not too far from the electronic spin, i.e. second or third neighbours. A small difference in the average distance from the chromium ion to fluorine and from chromium to lithium or sodium (this is logical given their different role in the sample structure) would explain our results. As far as the intensity differences between Na and Li peaks are concerned, these are due to the suppression effect associated with the first–second pulse delay, τ.

The fact that the ESEEM signal does not depend on the concentration of chloride or bromide ions allows more information to be gathered. Legein's simulations [17, 18] indicate that chromium clusters would not give an EPR signal which differs from that of the isolated chromium. In a sample with a high concentration of chloride or bromide ions, almost all the fluorine sites around chromium are occupied by heavier halide ions. In a chromium cluster, the second and third neighbours of chromium would belong to another chromium octahedron. This would lead to a very low concentration of fluoride ions as second and third neighbours. In such a case, the intensity of the peak at 5.2 MHz in samples with high concentrations of chloride and bromide ions would be reduced. As we do not see such behaviour, the ESEEM measurements indicate that chromium centres are mainly isolated.

5. Conclusions

A CW EPR and ESEEM spectroscopic study of chromium-doped fluoro-chlorozirconate and fluoro-bromozirconate glasses as a function of the glass composition has been performed.

The CW EPR data indicate a gradual change in the local environment of the transition metal, which suggests a preferential bonding of the heaviest halogen with the dopant. This is in agreement with previous interpretations of the optical properties of these materials.

In addition, the ESEEM signal shows two peaks, at the Larmor frequencies of ^{19}F and alkali metal nuclei (^{7}Li, ^{23}Na). The relative intensities of both peaks are independent of both the glass composition and the chromium content. This strongly indicates that chromium ions are mainly isolated, as has been proposed by Legein *et al* [17, 18], and is evidence against the formation of chromium clusters over extended ranges as was previously proposed [16] for fluorozirconate glasses.

Acknowledgment

Support for this work has been received from the DGICYT (Spain) under contract PB94-0550.

References

[1] Poulain M, Lucas J and Brun P 1975 *Mater. Res. Bull.* **10** 243
[2] Almeida R M (ed) 1987 *Halide Glasses for Infrared Fiberoptics (NATO ASI Series E-123)* (Dordrecht: Nijhoff)
[3] France P W, Carter S F and Parker J M 1986 *Phys. Chem. Glasses* **27** 32
[4] Suzuki Y, Sibley W A, El Bayoumi O H, Roberts T M and Bendow B 1987 *Phys. Rev.* B **35** 4472
[5] Cases R, Buñuel M A, Alcalá R and Orera V M 1993 *Proc. 12th Int. Conf. on Defects in Insulating Materials* ed O Kannert and J M Speath (Singapore: World Scientific) p 905
[6] Elyamani A, Poulain M, Saggese S J and Sigel H Jr 1990 *J. Non-Cryst. Solids* **119** 187
[7] Takahashi M, Yamamoto R, Kanno R and Kawamoto Y 1995 *J. Phys.: Condens. Matter* **7** 4583
[8] Takahashi M, Kanno R, Kawamoto Y and Kadono K 1995 *J. Phys.: Condens. Matter* **7** 7797
[9] Inoue H, Soga K, Makishima A and Yasiu I 1995 *Phys. Chem. Glasses* **36** 1
[10] Kawamoto Y, Kanno R, Yokota R, Takahashi M, Tanabe S and Hirao K 1993 *J. Solid State Chem.* **103** 334
[11] Buñuel M A, Alcalá R and Cases R 1995 *Radiat. Eff. Defects Solids* **135** 23
[12] Buñuel M A, Orera V M, Alcalá R and Cases R 1996 *10th Int. Symp. on Non-oxide Glasses* (New York: Corning)
[13] Buñuel M A 1997 *Doctoral Dissertation* University of Zaragoza
[14] Buñuel M A, Cases R, García J, Proietti M G and Solera J A 1997 *J. Physique IV* **7** 1219
[15] Dikanov S A and Tsvetkov Yu D 1992 *Electron Spin Echo Envelope Modulation (ESEEM) Spectroscopy* (Boca Raton, FL: Chemical Rubber Company) chs 6 and 7
[16] Harris E A 1987 *Phys. Chem. Glasses* **28** 196
[17] Legein C, Buzaré J Y, Emery J and Jacoboni C 1995 *J. Phys.: Condens. Matter* **7** 3853
[18] Legein C, Buzaré J Y, Boulard B and Jacoboni C 1995 *J. Phys.: Condens. Matter* **7** 4829
[19] Reijerse E J, Shane J J, de Beer E and Collison D 1989 *Electron Magnetic Resonance of Disordered Systems I* ed N D Yordanov (Singapore: World Scientific) pp 189–204
[20] Abragam A and Bleaney B 1970 *Electron Paramagnetic Resonance of Transition Ions* (Oxford: Oxford University Press) ch 19
[21] Oliete P B, Orera V M and Alonso P J 1996 *Phys. Rev.* B **54** 12 099